Article:

eprints@whiterose.ac.uk
https://eprints.whiterose.ac.uk/

1 **Removal of organic matter from reservoir water: mechanisms underpinning surface**

2 **chemistry of natural adsorbents**

3 Short title: Fuller's earth for treating surface water

4

5 Sabir Hussain [a] *, John van Leeuwen [a, c], Rupak Aryal [a], Binoy Sarkar [c] *, Christopher W.K.

6 Chow [a b], Simon Beecham [a]

7

8 [a] Natural and Built Environments Research Centre, School of Natural and Built Environments,

9 University of South Australia, Mawson Lakes, SA 5095, Australia.

10 [b] Australian Water Quality Centre, South Australian Water Corporation, Adelaide, SA 5000,

11 Australia.

12 [c] Environmental Science and Engineering Strand, Future Industries Institute, University of South

13 Australia, Mawson Lakes, SA 5095, Australia.

14

15

16

17

18

19

20 * Corresponding authors:

21 B. Sarkar; e-mail: binoy.sarkar@unisa.edu.au

22 S. Hussain; e-mail: sabir.hussain@mymail.unisa.edu.au

23 **Graphical abstract**

24

The graph shows UV @ 260nm (y-axis, 0.000 to 0.040) versus Apparent molecular weight 'AMW' (Dalton) (x-axis, 100 to 100000). Legend: AMW Profile Raw water, AMW Profile FE, AMW Profile SQ, AWM profile-MSQ. Labels point to Raw water, SQ, MSQ, FE. Marked "a".
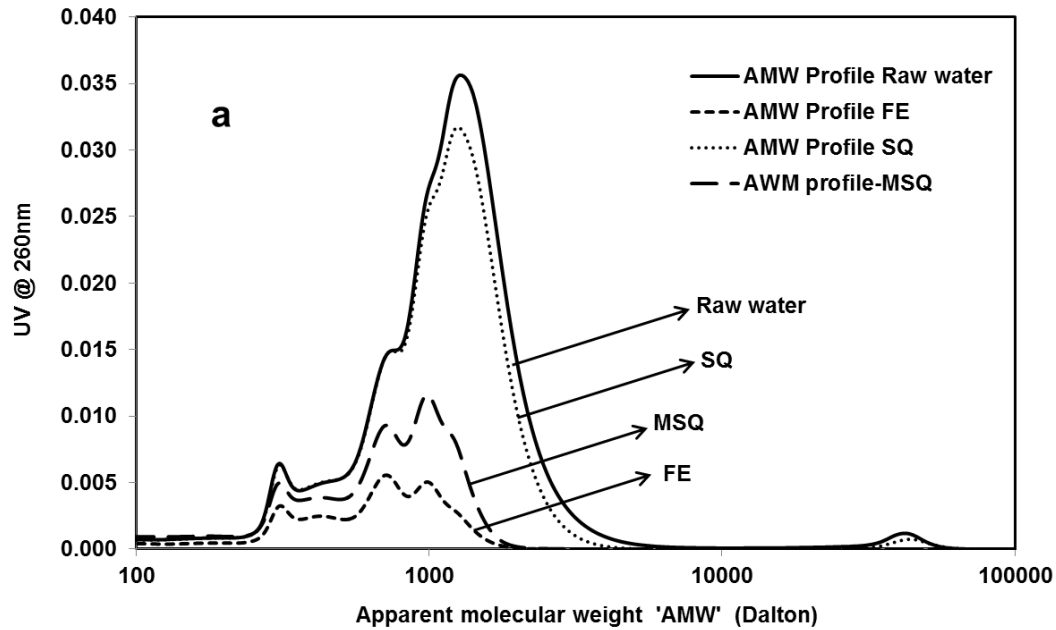
25

26

27 **Highlights**

28 • Fuller's earth (FE), natural and modified quartz were studied for DOC removal from reservoir

29 water.

30 • FE yielded greater DOC removal at broad range of pH and at low dose than quartz sand.

31 • F-EEM and HPSEC showed higher removal of humic substance and low AMW compounds.

32 • Adsorption data best fitted to Freundlich model, indicating multilayer adsorption.

33 • Pseudo-second-order kinetic model fitting indicated a chemisorption process.

34

Abstract

One of the key challenges in water treatment industry is the removal of organic compounds by cost-effective methods. This study evaluated the adsorptive removal of dissolved organic carbon (DOC) from reservoir water using fuller's earth (FE) in comparison with natural (SQ) and modified quartz (MSQ) sands. The removal capacities of FE at different contact times, pH levels, adsorbent dosages and initial DOC concentrations were compared with both the quartz sands. The optimum DOC removals by FE and SQs were achieved at contact time of 60 min and 30 min, pH level of 6 and 4, and at adsorbent dose of 1.5 g/150 mL and 10 g/100 mL, respectively. The adsorption capacity of FE (1.05 mg/g) was much higher compared to the MSQ (0.04 mg/g) and SQ (0.01 mg/g). Adsorption equilibrium data better fitted to the Freundlich model than the Langmuir model, suggesting that adsorption occurred primarily through multilayer formation onto the surfaces of FE and SQ. The pseudo-second-order model described the uptake kinetics more effectively than the pseudo-first-order and intra-particle diffusion models, indicating that the mechanism was primarily governed by chemisorption. These observations were well supported by the physiochemical characteristics and charge behaviour of the adsorbents. In mass-transfer study, the results of liquid film diffusion model showed that the adsorption of DOC on FE was not controlled by film diffusion, but other mechanisms also played an essential role. This study demonstrates that FE is an effective adsorbent for the removal of DOC in surface water treatment.

Keywords: Adsorption; Fluorescence spectroscopy; Isotherm and kinetics; Liquid film diffusion; Water treatment.

1. Introduction

Dissolved organic matter (DOM) in natural waters is a complex heterogeneous mixture of naturally occurring organic constituents such as humic and fulvic acids that are coloured, aromatic and hydrophobic in nature. It also comprises of low molecular weight organics that are hydrophilic in nature, including aliphatic and nitrogenous compounds such as amino acids, carbohydrates and proteins (Matilainen et al. 2011). DOM, measured as dissolved organic carbon (DOC) in surface waters, has increased considerably in the last couple of decades in many regions of the world, likely because of the exacerbation of environmental issues such as global warming, intensification of drought and rain events, and soil acidification (Forsberg 1992; Korth et al. 2004; Worrall and Burt 2007). The presence of DOC in drinking water can cause significant problems to water supply utilities because it can produce unpleasant colour, taste and odour, and may act as substrate for microbial growth in distribution systems. It may increase coagulant or disinfectant demands, foul membrane's surface and clog activated carbon pores, which deteriorate the treatment performance. If not removed adequately by the treatment process, higher levels of chlorine used for disinfection may react with residual DOC to form disinfection by-products (DBPs) such as trihalomethanes (THMs), and these can be of serious health concerns (Collins et al. 1986; Tang et al. 2016).

Traditionally, DOC removal from drinking water has been accomplished by coagulation (Deegan et al. 2011; Hussain et al. 2014; Matilainen et al. 2010; Rahbar et al. 2006). However, more recently, a shift is evident towards adsorption with activated carbon (Bonvin et al. 2016; Dastgheib et al. 2004; Matilainen et al. 2006), ion-exchange resins (Arias-Paic et al. 2016; Humbert et al. 2005; Kitis et al. 2007) and membrane filtration technologies (Van der Bruggen et al. 2003; Yang et al. 2014). In coagulation, one of the main disadvantages is the handling of

80   sludge and its disposal. In addition, adsorption with activated carbon and use of membrane filters

81   are cost intensive; and desorption by ion-exchange resins also cause disposal problems for large

82   amounts of concentrated waste brine produced during the process. This showed that the removal

83   of organic matter by cost-effective methods is still one of the key challenges in water treatment

84   industry. As a result, efficient and cost effective adsorbents are actively sought by scientists and

85   water industries around the world. One of the main advantages of using natural or modified

86   adsorbents over traditional water purification methods is that these materials may be easily

87   regenerated and reused during the water treatment process (Chow et al. 2009).

88   Fuller's earth (FE), a natural clay material also known as 'bleaching earth', has been successfully

89   used for the removal of heavy metals (Oubagaranadin et al. 2007), bleaching of crude edible oil

90   (Mana et al. 2008), dyes (Atun et al. 2003) and polyvinylalcohol (Bajpai and Vishwakarma

91   2003) due to its low cost, high surface area and abundant availability. The current approaches are

92   well established with the use of activated carbon and anion exchange resins for DOM removal,

93   but the findings on the potential use of FE is still limited. The functional relationship between the

94   physiochemical characteristics of this natural adsorbent and plausible mechanism for DOC

95   removal is also largely unknown. Therefore, this work was emphasised on the potential

96   application of natural fuller's earth in surface water treatment. For this purpose, FE's results

97   were compared with the natural and modified quartz sands which were earlier reported as an

98   effective material for organic matter removal from water (Hedegaard and Albrechtsen 2014;

99   Jarvis and Majewski 2012). The present study was aimed (1) to examine the DOC removal

100 capacity of FE in comparison with SQs at different contact times, pH levels, adsorbent dosages

101 and initial DOC concentration, and (2) to empirically predict the mechanisms of DOC removal

102 by these adsorbents in relation to their physiochemical characteristics. This research was

5

103   conducted at the Natural and Built Environments Research Centre, School of Natural and Built

104   Environments, University of South Australia, Mawson Lakes, Australia during Oct 2014-May

105   2015.

106

107   **2.   Materials and Methods**

108   2.1.   Water collection and analysis

109   Water samples were collected from the inlet point of the water treatment plant of Myponga

110   Reservoir in South Australia. All samples were stored in a cold room at 4°C prior to the batch

111   experiments. DOC was measured using a total organic carbon analyser (Model 820, Sievers

112   Instruments Inc., USA). UV absorbance (at 254 nm) and true colour calibrated by 50 HU Cobalt

113   Platinum standards (at 456 nm) were determined using a UV-120 UV-Vis spectrophotometer

114   (MIOSTECH Pty Ltd., Australia). A portable pH meter (TPS, Model WP-91) was used to

115   measure the pH of raw and treated waters. The water quality was as follows: DOC, 12.5 ± 0.2

116   mg/L; UV_{254nm}, 0.444 ± 0.005/cm; specific UV absorbance (SUVA), 3.6 L/mg.m; colour, 43 ± 2

117   HU; specific colour, 3.4; turbidity, 1.9 ± 0.1 NTU; pH, 7.4 ± 0.2 and alkalinity of the raw water,

118   108 mg/L as $CaCO_3$.

119   For DOM characterisation, high performance size-exclusion chromatography (HPSEC) and

120   fluorescence excitation-emission matrix (F-EEM) spectroscopy were employed. HPSEC

121   technique was used to determine the apparent molecular weight (AMW) profile of DOM present

122   in raw and treated waters as described by Chow et al. (2008). F-EEM spectra were acquired

123   using a Perkin–Elmer LS55 fluorescence spectrophotometer. The fluorescence intensities of

124   DOM composition corresponding to F-EEM regions I, II, III, IV and V, and referred to as

125   Protein 1 (P1), Protein 2 (P2), fulvic acid (FA), soluble microbial products (SMP) and humic

126 acid (HA) like compounds, respectively, were calculated adopting the method as described by

127 Chen et al. (2003). The sum (total) and mean fluorescence intensities of P1, P2, FA, SMP and

128 HA regions were determined based on the total number of data points (N) of these regions as

129 1000, 1000, 2880, 840 and 4800, respectively. The total fluorescence intensities of P1, P2, FA,

130 SMP and HA regions for the surface waters were about 109, 644, 3533, 268 and 3972 arbitrary

131 units (au), whereas the mean intensity values of the corresponding regions were about 0.1, 0.58,

132 1.27, 0.27 and 0.78 units, respectively. The higher fluorescence intensities of HA and FA-like

133 compounds indicated that the reservoir water was mainly comprised of humic substances. Gone

134 et al. (2009) also reported that these compounds (HA and FA) are the common fluorophores in

135 natural surface water.

136

137 2.2.   Adsorbent characterisation

138 The FE and SQ were supplied by Ace Chemical Company and Unimin Australia Pty. Ltd.

139 (Adelaide, South Australia), respectively. Both adsorbents were oven dried at 50°C prior to the

140 adsorption study. The surfaces of SQ were modified with allylamine compound ($C_3H_5NH_2$) by

141 plasma polymerization method as discussed in (Jarvis and Majewski 2012). Therefore, the

142 modified SQ was named as MSQ. Das et al (2013) also reported similar approach for the

143 removal of perfluorooctane sulfonate compounds from water using oleylamine-modified clay

144 adsorbent. The structural and surface chemical characteristics of FE and SQs were determined

145 using scanning electron microscopy (SEM), Fourier transform infrared (FTIR) spectroscopy, and

146 thermo-gravimetric analysis (TGA). Surface area and pore size distribution were determined

147 using N_2 adsorption measurements at liquid nitrogen temperature by Gemini 2380 surface area

148 analyser (Micrometrics, USA) (Table 1). The SEM images of FE and SQs were taken in high

149   vacuum mode and with a 20kV accelerating voltage by an Everhart-Thornley Detector (ETD) or

150   Large Field Detector (LFD) using a FEI Quanta 450 FEG Environmental Scanning Electron

151   Microscope. The elemental composition of the samples were analysed by energy dispersive x-ray

152   spectroscopy (EDX) using an Apollo EDX detector (EDAX®, USA).

153   For FTIR analysis, the samples were ground and mixed homogenously with dehydrated KBr and

154   pressed into discs. Infrared (IR) spectra were acquired using an Agilent Cary 600 Series FTIR

155   Spectrometer over spectrum wavenumbers 4,000-400 cm^{-1}. The spectrum range was obtained by

156   the co-addition of 64 scans with a resolution of 4 cm^{-1}. (Bajpai and Vishwakarma 2003) also

157   adopted a similar range of spectrum (4,000-400 cm^{-1}) in studying the adsorption of

158   polyvinylalcohol onto FE surfaces. Thermogravimetric analysis (TGA) was performed using a

159   Mettler-Toledo-TGA/DSC1 instrument (Mettler-Toledo International Inc.). The temperature for

160   TGA was raised from 25 to 900°C at a heating rate of 10°C/min with a resolution of 6°C under

161   N_2 flow (70 mL/min).

162

163   2.3.   Batch experiments

164   Batch experiments of FE and SQs were conducted to study the effect of key parameters on the

165   DOC removal. This was done at the following experimental conditions: contact time: 2–240 min;

166   pH levels: 4–11; adsorbent doses: 0.05–15 g/150mL for FE and 1–40 g/100mL for SQs; and

167   initial DOC concentration: 6.8–80 mg/L. A series of conical flasks containing a known volume

168   of raw water were agitated at a pre-determined agitation speed of 300 rpm on an orbital shaker.

169   The desired concentration of DOC was acquired by adding fulvic acid (FA), supplied by Omnia

170   (Nutriology) Specialties Australia Pty Ltd, Australia, in tested surface waters. The FA used in

171   this study was extracted from a natural aged humus and concentrated into a completely soluble

172   dry powder which contains about 70% fulvic acid, 5% humic acid, 18% potassium and 4%

173   nutrients. The stock solution (2000 mg/L) of FA was prepared by dissolving 2 g of FA into 1 L

174   high purity Milli-Q water. The pH of tested water was adjusted by 0.2 M HCl or 0.2 M NaOH

175   solutions. For kinetic study, the time required for reaching the equilibrium condition was

176   determined by withdrawing the treated water samples of individual flask at different time

177   intervals. Immediately after this, the treated water samples were filtered through 11 µm

178   Whatman No. 1 filters, followed by 0.45 µm and 0.22 µm syringe filters. The filtrates were

179   further analysed for the measurement of final DOC, UV_{254nm} and colour. The percentage removal

180   of each parameter was determined using the following equation (Eq. 1):

181 $$Removal \; (\%) = \frac{(C_i - C_e) \times 100}{C_i} \qquad \qquad \text{(Eq. 1)}$$

182   Where, C_i and C_e are the initial and final concentrations of water parameters (such as DOC in

183   mg/L), respectively.

184

185   2.4.   Adsorption equilibrium and kinetic studies

186   Adsorption equilibria and rate data are the essential requirements in designing an adsorption

187   system. Adsorption studies were carried out by varying the adsorbent dosages at pre-determined

188   optimum conditions. The equilibrium adsorption capacities were evaluated at contact time higher

189   than 60 min, when the equilibrium condition was reached. The DOC adsorption data were

190   analysed by fitting to Langmuir, Freundlich, Temkin and Dubinin-Redushkevich models. The

191   linear equations of these models were used to assess the best-fit model and to determine the

192   adsorption mechanisms of DOC as either monolayer or multilayer formation onto the adsorbent

193   surfaces. The suitability of each model was determined by linear regression (comparison of

194   coefficient of determination, R^2) from the experimental data. The equilibrium adsorption

195   capacity or q_e (mg/g) was calculated as follows (Eq. 2):

196    $$q_e = \frac{(C_i - C_e) \cdot V}{m}$$ (Eq. 2)

197   Where, C_i and C_e are the initial and final concentration of DOC (mg/L), V is the volume of

198   surface water (mL) and m is the mass of adsorbent (g).

199   Kinetics of DOC adsorption by FE, MSQ and SQ were investigated as a function of time by four

200   different kinetics models, i.e., pseudo-first-order, pseudo-second-order, intra-particle diffusion

201   and liquid film diffusion model. The coefficient of determination values of each model were

202   obtained from the linear plots. The experimental q_e values of pseudo-first-order and pseudo-

203   second-order models were compared with the calculated q_e values to assess the best fit model.

204

205   **3.   Results and Discussion**

206   3.1.   Physiochemical characteristics of adsorbents

207   The SEM micrographs of FE, MSQ and SQ were shown in Fig. 1. The outer surface of all three

208   adsorbents show crystalline forms with honeycomb apertures. However, the FE images exhibited

209   greater surface area and porous surfaces than the SQs. The particle morphology of FE was more

210   irregular and comprised aggregates of microcrystalline plates while the surfaces of SQs were less

211   irregular and towards singular (not aggregate) particle. The FTIR spectra of the adsorbents are

212   shown in Fig. 2. The IR spectra of FE exhibited broad bands at about 1000 cm⁻¹ and 3500 cm⁻¹,

213   indicating the presence of both free and hydrogen bonded OH groups (Socrates, 2004). These

214   spectra mark the presence of silanols with Si-O stretching and aluminols with Al-O stretching at

215   1000 cm⁻¹ and 3500 cm⁻¹ in FE (Gu et al., 2011). In addition, the strong band at around 1700 cm⁻

216   ¹ of the spectra also indicates the presence of carboxylate anion and asymmetrical stretching of

217 C=O. However, FTIR spectra for SQs showed weak bands at 3500 cm^{-1} and strong bands at 1000

218 cm^{-1}, indicating lack of Al-O stretching as observed in FE. The peaks at around 775 cm^{-1} and 795

219 cm^{-1} are doublets of quartz which show Si-O stretching (Perelomov et al. 2016). In addition, Fig.

220 2 showed the clear doublet for sands, but not for FE because quartz contents in FE are less than

221 SQ. The SEM-EDX elemental analysis showed that the FE was mainly composed of O (50.2%),

222 C (21.7%), Si (15.5%), Al (7.2%), Ca (2.4%), Na (2.7%) and others (0.4%), whereas, the SQs

223 were mainly composed of Si (65-67%), O (32-35%) and Al (0.3-0.4%). TGA curves of the FE,

224 MSQ and SQ were used to quantify the weight loss with increasing temperature. The first weight

225 loss at around 100-115°C corresponded to the dehydration of physical water present in all

226 adsorbents. The second weight loss in FE at 500°C might be due to the loss of organic content

227 present in the adsorbent itself. The sharp weight loss of MSQ at 280°C was probably due to the

228 loss of its polymerized allylamine coating from the material's surface (Sarkar et al., 2010a;

229 2010b). It was also observed that both SQ (after 110°C) and MSQ (after 280°C) slightly gained

230 some weight with increasing temperature, reflecting possible oxide formation.

231

232 3.2.   Process parameters for DOC removal

233 3.2.1   Effect of contact time

234 The effect of different contact times on adsorptive removal of DOC using 1g/150mL of FE and

235 5g/100mL of SQs at neutral pH are shown in Fig.3. In the case of FE, it was evident that there

236 was a rapid removal of DOC within the first few minutes and the equilibrium was reached at a

237 contact time of 60 min, after which the removals of UV$_{254nm}$ and colour and DOC remained

238 unchanged. The initial rapid adsorption followed a very slow approach to equilibrium, and

239 therefore, contact time of 60 min was considered as optimum time. The removal efficiencies at

240   contact time of 60 min were about 43%, 64% and 85% for DOC, UV_{254nm} and colour,

241   respectively. These were significantly higher than the removals of these components by SQ (6%,

242   10% and 13%, respectively) and MSQ (19%, 17% and 38%, respectively) at a contact time of 30

243   min, which was found to be the optimum contact time for both sands. Based on these results, the

244   subsequent experiments were conducted using 60 and 30 min contact times for FE and SQs,

245   respectively.

246

247   3.2.2.   Effect of initial pH

248   The removal of DOC was examined over a pH range of 4-11 (Fig. 4). Adsorption characteristics

249   of the adsorbents were highly pH dependent. The results show that the percentage removal of

250   DOC was decreased as the initial pH of water solution increased. This was likely because the

251   adsorbent surfaces at pH < 7 became more positively charged due to protonation, leading to the

252   adsorption of negatively charged DOC on the FE's surface at lower pH conditions. Such

253   protonation reactions commonly occur on mineral surfaces having variable charges (Rusmin et

254   al. 2016; Sarkar et al. 2011). The maximum adsorptive removals for FE were achieved over a pH

255   range 4–6. The final pH levels of the treated waters were in the range of 3.4–3.8. The optimum

256   pH for DOC removal by FE was determined to be at pH 6, at which more than 90% of colour,

257   55% of DOC and 73% of UV_{254nm} were removed. FE had almost no effect on the removal of

258   DOC and colour at pH > 9. Removal of DOC by FE was near to zero or negative at highly

259   alkaline conditions (pH ≥ 10), also indicting at high pH, the solubilisation of particulate organic

260   matter had occurred or naturally occurring organic matter present on/in the adsorbent material

261   got desorbed into the aqueous phase. At this high pH, the variably charged adsorbent surface also

262   became negatively charged as a result of deprotonation (Rusmin et al. 2016; Sarkar et al. 2011),

263 which consequently would impart a repulsive force to the negatively charged DOC molecules

264 and decrease adsorption capacity. In addition, the TGA results of FE (Fig. 2) showed that there

265 was significant weight loss at temperatures between 400 and 500°C, which might be partially

266 due to the loss of organic matter present within the FE. To confirm this, 1 g of FE was agitated in

267 150 mL solution of high purity Milli-Q water at pH 11 for 1 h. DOC concentration in the clear

268 supernatant was found to be approximately 4.3 mg/L. Also, the EEM spectra of this solution

269 confirmed the presence of high fluorescence intensities of FA and HA compounds (figure not

270 shown). The above results clearly showed that at high pH conditions ($\geq$10), FE did not adsorb

271 DOC.

272 The zeta potential and electrophoretic mobility values of FE decreased significantly from +0.8 to

273 -41 mV and -1.2 to -3.3 μm.cm/Vs, when the pH was increased from 1 to 11. The point of zero

274 charge (pzc) or isoelectric point (IEP) of both FE and SQ were near to pH 2.0 and 5.1,

275 respectively. The IEP values of the SQs used in this study were previously documented by

276 (Jarvis and Majewski 2012). They reported that IEP of MSQ increased by modifying the surface

277 of SQ. In general, the adsorbent surface was positively charged at pH below the IEP whereas the

278 surfaces were generally negatively charged at pH above the IEP. For SQs, the maximum

279 removals of DOC, colour and UV_{254nm} were achieved at pH 4, thus the optimum pH for both

280 quartz sands was chosen as pH 4. The removals achieved by SQs were much lower in

281 comparison to the removal achieved by FE. Subsequent experiments were conducted at pH 6 for

282 FE and at pH 4 for SQs.

283

284 3.2.3. Effect of adsorbent dose

285   The effects of adsorbent dose on the removals of DOC, colour and UV_{254nm} are shown in Fig. 5.

286   FE was used at dosages ranging from 50 mg-15 g/150 mL while SQs were used at levels

287   between 1-40 g/100 mL. The increase in the FE dose up to 1.5 g FE/150 mL surface water

288   resulted in rapid increase in DOC removal, but at higher dose, further removals were minimal,

289   indicating equilibrium condition had been reached. At 1.5 g/150 mL of FE, the removals of

290   DOC, colour and UV_{254nm} were found to be 56%, 94% and 79%, respectively. At this dose, the

291   specific UV absorbance (SUVA) value of treated water decreased to 1.8 L/mg.m from the initial

292   value of 3.6 L/mg.m, indicating most of the hydrophobic compounds were removed by FE. In

293   case of SQs, a dose between 5 -10 g/100 mL surface water was required to achieve the maximum

294   DOC removal (Fig. 5b). For SQ, the removal efficiencies of DOC, colour and UV_{254nm} were

295   approximately 14%, 37% and 17%, whereas for MSQ these values were approximately 31%,

296   70% and 29%, respectively. The SUVA values of treated waters were found to be more than 3.2

297   at all dosages, indicating that treated water was still hydrophobic in nature. Thus, the DOC

298   removal achieved by FE was significantly greater than the SQs. For subsequent experiments, the

299   FE dose of 1.5g /150 mL and, 10 g/100 mL dose of SQs were chosen as optimum dosages.

300

301   3.2.4.   Effect of initial DOC concentration

302   DOC removal efficiencies gradually decreased when the initial DOC concentration was

303   increased for all adsorbents tested at their optimum dosages (Fig. 6). The results showed that the

304   dose of 3 g/150 mL of FE was able to remove about 90% of colour, 80% of UV_{254nm} and more

305   than 70% of DOC even at the initial DOC concentrations exceeding 25 mg/L. This probably

306   occurred as a result of decrease in adsorbate to adsorbent ratio, resulting in the increase of

307   available number of surface sites for adsorption. Comparatively, DOC removals achieved by SQs

308 were very low when initial DOC concentration exceeded 20 mg/L, with removal efficiencies

309 below 20%.

310

311 3.3. DOM characterisation in treated water

312 F-EEM spectroscopy was employed to evaluate the DOM composition of raw and treated waters.

313 The EEM spectra of five regions, P1, P2, FA, SMP and HA (as detailed in Section 2.1) are

314 shown in Fig. 7. Total fluorescence intensities (FI) of P1, P2, FA, SMP and FA for the FE treated

315 water were about 80, 314, 996, 131 and 773 units, respectively. For MSQ, the corresponding

316 total FI were about 24, 256, 2548, 130 and 2904 units, whereas for SQ, intensities were about 35,

317 304, 2724, 144 and 3168 units, respectively. In addition, the mean FI of P1, P2, FA, SMP and

318 HA for the FE treated water were about 0.07, 0.28, 0.32, 0.13 and 0.15 units, respectively. For

319 MSQ, the corresponding mean FI were about 0.02, 0.23, 0.81, 0.13 and 0.57 units, whereas for

320 SQ, these were about 0.03, 0.27, 0.87, 0.15 and 0.63 units, respectively. The above results

321 indicate that the mean FI of P1, P2 and SMP of treated waters for the three adsorbents tested

322 were almost the same compared to the mean FI of FA and HA. Gone et al. (2009) demonstrated a

323 linear relationship between the different fluorescence peak (namely A, C and T) intensities and

324 DOC percentage removal, and found that the decrease in organic matter fluorescence intensity

325 can be used as a simple technique for the prediction of DOC removal (Gone et al. 2009). The

326 maximum removals of total FI of HA and FA achieved by FE were 86% and 71% compared to

327 the removals achieved by MSQ (27% and 28%) and SQ (20% and 23%), respectively. The

328 results showed that the FE yielded higher removal of humic acids-like compounds whereas SQs

329 yielded higher removals of proteins-like compounds (P1 and P2) than the FE.

15

330   The selective removals of organic compounds of specific apparent molecular weights (AMW)

331   were determined by partitioning the AMW profile into four zones, Zone 1 (100-500 Da), Zone 2

332   (500-2,000 Da), Zone 3 (2,000-10,000 Da) and Zone 4 (10,000-70,000 Da). The relative

333   abundances of organics with AMWs within zones 1, 2, 3 and 4 in raw water were 11.2%, 75.3%,

334   10.8% and 2.7%, respectively. This indicates that organics in the AMW range of 600-2,000 Da

335   were the most dominant in raw water. Each adsorbent showed different removal efficiency at its

336   particular optimum condition. The HPSEC results indicate that FE can remove between ~ 50

337   to100% of UV absorbing organic compounds in the range of 100–70,000 Da, whereas the

338   removal rates of MSQ and SQ for the same range of AMW were ~13–100% and ~0.3–55%,

339   respectively, depending on the molecular weight (Fig. 8). This indicates that FE is more efficient

340   for the removal of low molecular weight organic compounds than MSQ, and SQ shows the

341   lowest removals for all zones.

342   3.4.   Adsorption isotherms

343   Isothermal modelling is commonly employed to relate the capacity of adsorbate removal by the

344   adsorbent and to describe the mechanisms by which adsorption occurs at the interface. The

345   adsorption experimental data were analysed using linear forms of Langmuir, Freundlich, Temkin

346   and Dubinin-Redushkevich (D-R) isotherm models, based on the linearized coefficient of

347   determination (Supplementary Information: Fig. S1). The Langmuir model assumes that the

348   adsorption occurs primarily by saturated monolayer formation of the adsorbate on the surface of

349   adsorbent with no lateral interaction between the adsorbed molecules, and is based on surface

350   homogeneity having equal energy. The Langmuir equation (Langmuir 1918) is expressed as (Eq.

351   3):

352   $$q_e = \frac{abC_e}{1+aC_e}$$ (Eq. 3)

353 The linear form of the Langmuir isotherm model is (Eq. 4):

$$\frac{1}{q_e} = \frac{1}{abC_e} + \frac{1}{b}$$ (Eq. 4)

355 Where, q_e is the adsorption capacity (mg/g); a (L/mg) is the Langmuir constant and is indirectly

356 related to the enthalpy of adsorption; b (mg/g) is the maximum sorption capacity for monolayer

357 coverage of the adsorbent, and C_e (mg/L) is the equilibrium concentration of adsorbate in the

358 solution. The values of a and b were determined from the slope and intercept of plot of $1/q_e$ vs.

359 C_e (Supplementary Information: Fig. S1a). The Langmuir constant '*a*' value of FE was greater

360 than the SQs, which indicated the affinity of FE towards DOC. However, the negative values of

361 the Langmuir constants 'a' and 'b' (Table 2) reflected the inadequacy of this isotherm model for

362 describing the adsorption process despite it showed a considerable linearity for data fitting

363 (correlation coefficient, R^2 ranging from 0.68 to 0.98). Additionally, a dimensionless constant,

364 separation factor or equilibrium parameter, R_L (Eq. 5), was calculated using the Langmuir

365 constant and was used to determine the adequacy or inadequacy of this model.

$$R_L = \frac{1}{1+aC_i}$$ (Eq. 5)

367 Where, 'C_i' is the initial concentration of DOC, and 'a' is the Langmuir constant. The R_L values

368 between 0 to 1, 0 and > 1 indicate favourable, irreversible and unfavourable adsorption,

369 respectively (Fierro et al., 2008; Bhatt et al., 2012). In the current study, R_L values of FE and SQ

370 were > 1. The negative value of '*a*' for DOC adsorption onto FE yielded the R_L value > 1

371 (unfavourable adsorption). This further showed the inadequacy of fitting of the Langmuir model

372 to the adsorption data.

373 The Freundlich model (Freundlich 1926) is employed to describe surface heterogeneity, and can

374 be expressed as (Eq. 6):

375 $$q_e = K_f C_e^{1/n} \qquad \text{(Eq. 6)}$$

376 The linear form of above equation is (Eq. 7):

377 $$log\ q_e = log\ K_f + \frac{1}{n}\ logC_e \qquad \text{(Eq. 7)}$$

378 Where, K_f (mg/g) is the Freundlich affinity coefficient and refers to the adsorption capacity and

379 n (dimensionless) is the Freundlich exponential coefficient, whose value can depend on

380 adsorbent types and experimental pH values. Generally, the adsorption strength increases as the

381 value of n decreases and the adsorption capacity decreases as K_f decreases (Hyung and Kim

382 2008). The values of K_f and n were determined from the plot of log q_e vs. log C_e (Supplementary

383 Information: Fig. S1b). In this study, the n and K_f values of FE were much greater than both SQs

384 (Table 2). The Freundlich and Langmuir isotherm models' parameters and correlation

385 coefficients values of FE, MSQ and SQ were given in Table 2. The Langmuir constant '*a*' value

386 of FE was greater than the SQs, which described as an indication of the affinity of FE towards

387 DOC. The adsorption data of FE closely fitted to the Freundlich model ($R^2 = 0.99$), followed by

388 Langmuir model ($R^2 = 0.98$).

389 Temkin model is used to determine the heat of adsorption and the adsorbent-adsorbing species

390 interactions. Temkin model can be expressed as follows (Eq. 8):

391 $$q_e = \frac{RT}{b}\ln(K_T C_e) \qquad \text{(Eq. 8)}$$

392 The linearized form of above equation is (Eq. 9):

393 $$q_e = B_1\ln K_T + B_1\ln C_e \qquad \text{(Eq. 9)}$$

394 Where, B_1 is related to heat of adsorption which is equal to RT/b; R Universal gas constant

395 (8.314 J/mol.K); T absolute temperature (K). The constants B_1 and K_T (L/mg) were determined

396 from the plot of q_e vs. ln C_e (Supplementary Information: Fig. S1c). The values of B_1 for FE and

397 MSQ were found to be 4.40 and 1.89, respectively whereas the K_T values for FE and MSQ were

398 found to be 0.20, and 3.72, respectively. It was observed from the values of B_l and K_T that heat of

399 adsorption for FE is greater than MSQ whereas the binding energy for FE is lower than MSQ.

400 Dubinin-Redushkevich (D-R) adsorption isotherm is expressed as follows (Eq. 10):

401
$$q_e = q_m \exp(-Be^2) \qquad \text{(Eq. 10)}$$

402 The linear form of the D-R equation is (Eq. 11):

403
$$ln\ q_e = \ln q_m - Be^2 \qquad \text{(Eq. 11)}$$

404 Where, q_m is the theoretical monolayer saturation capacity (mg/g); e is known as Polanyi

405 potential and is equal to $e = RT\ ln(1 + \frac{1}{C_e})$. B is the constant of free adsorption energy (mg^2/J^2)

406 and E is the apparent adsorption energy (J/mg) which was calculated using the following

407 formula; $E = 1/\sqrt{2B}$. The value of E was derived from the slope and intercept of e^2 and $\ln q_e$

408 (Supplementary Information: Fig. S1d). Results obtained from the linear plot showed that the

409 value of mean free energy E of adsorption per molecule of adsorbate for FE (223.6 J/mg) was

410 much higher than MSQ (100 J/mg) and SQ (50 J/mg).

411 Overall, the R^2 value of Freundlich model for FE and MSQ was comparatively greater than the

412 R^2 values of Langmuir, Temkin and D-R isotherm models which explained multilayer

413 adsorption. These adsorption data suggested that DOC adsorption occurred primarily by

414 multilayer formation in arbitrary distribution due to heterogeneous energetic distribution of

415 active sites onto the FE and SQs surfaces.

416

417 3.5.   Adsorption kinetics

418 The adsorption kinetics of DOC by FE and SQs were investigated from the pseudo-first-order,

419 pseudo-second-order and intra-particle diffusion models. The pseudo-first-order kinetic model

420 assumes that the rate of change in adsorbate uptake is directly related to the difference in the

421 saturation and the amount of solute uptake in a given time, and models the rate of adsorption of

422 adsorbate onto the adsorbent (Lagergren 1898). This model was expressed in a linear form as

423 (Eq. 12):

424
$$\log(q_e - q_t) = \log q_e - k_1 t \qquad \text{(Eq. 12)}$$

425 Where, q_e and q_t are the adsorption capacity (mg/g) of the adsorbent at equilibrium and agitation

426 time t (min), respectively and k_1 is the pseudo-first-order rate constant (min^{-1}). The values of q_e

427 and k_1 were obtained from a linear plot of $\log (q_e - q_t)$ against contact time t (min), figure is not

428 shown here. The pseudo-second-order kinetic model proposed by (Ho and McKay 2000)

429 assumes that the chemisorption is the rate-limiting step, where the adsorption is due to physico-

430 chemical interaction. The linear form of this model is expressed as follows (Eq. 13):

431
$$\frac{t}{q_t} = \frac{1}{k_2 q_e^2} + \frac{1}{q_e t} \qquad \text{(Eq. 13)}$$

432 Where, k_2 (g (mg min)^{-1}) is the pseudo-second-order rate constant and all other parameters are

433 the same as detailed in Equation 12. The values of q_e and k_2 were obtained from the linear plot of

434 t/q_t versus agitation time (Supplementary Information: Fig. S2a). The intraparticle diffusion

435 model assumes that the adsorption process is diffusion-controlled and that the rate of adsorption

436 depends on the speed at which adsorbate diffuses towards the adsorbent which is expressed in

437 linear form using the following equation (Eq. 14):

438
$$q_t = k_3 t^{1/2} + C \qquad \text{(Eq. 14)}$$

439 Where, k_3 (g (mg/min)) is the intraparticle diffusion rate constant and C is the intercept. A linear

440 plot of q_t versus $t^{1/2}$ was used to obtain the values of k_3 and C (figure not shown).

441   The kinetic parameters determined for pseudo-first-order, pseudo-second-order and intra-particle

442   diffusion models, and the corresponding coefficient of determination for the adsorption of DOC

443   by FE, MSQ and SQ were presented in Table 2. The parameter values for each model indicate

444   that the adsorption rate was very fast for FE than the SQs. The results of pseudo-first-order

445   kinetic model indicated that the values of equilibrium adsorption capacities, q_e, did not agree

446   with the monolayer capacities determined by Langmuir equilibrium isotherm model and that the

447   plot of $\log(q_e - q_t)$ against time (t) was not truly linear, suggesting that the adsorption process did

448   not follow pseudo-first-order kinetics. When kinetic parameters along with R^2 for the pseudo-

449   second-order kinetic model were investigated, the agreement between experimental and

450   calculated equilibrium adsorption capacities, q_e, was evident. The plot of t/q_t versus agitation

451   time was highly linear and the R^2 value was very close to one. The experimental data was well

452   agreed with the pseudo-second-order model. The electrostatic attraction between the charged

453   surface of both adsorbents and DOM particles may be considered as the main adsorption

454   mechanism, suggesting DOC adsorption onto the adsorbents surfaces followed chemisorption

455   (Ho and McKay 2000; Rusmin et al. 2015).

456   When the intra-particle diffusion model was investigated, the regression of q_t versus $t^{1/2}$ was not

457   found to be linear and failed to pass through the origin. Instead, the plot reflected a large

458   intercept, suggesting greater boundary layer effect and contribution of the surface sorption in the

459   rate controlling step. These findings indicated that the intra-particle diffusion was not the sole

460   rate limiting step for the adsorption kinetics. The values of K_3 of this model for FE were greater

461   than SQs (Table 2). Furthermore, in mass-transfer study, the liquid film diffusion model,

462   (Oubagaranadin et al. 2007), was applied to determine the transfer behaviour of DOC molecule

463   to the solid phase boundary using the following equation (Eq. 15):

464
$$ln\,(1 - F) = -K_{fd}\,t \qquad\qquad\qquad (Eq.\ 15)$$

465 Where, F is the ratio of q_t/q_e and K_{fd} is the film diffusion rate constant. The parameters of this

466 equation are similar to Equation 11 (pseudo-first-order kinetics). The results obtained from the

467 linear plot (Supplementary Information: Fig. S2b) between -ln (1-F) vs. time (t), indicating that

468 the straight lines of liquid film diffusion line for FE and SQs did not pass through the origin

469 (zero) point. This indicates that the adsorption system for FE and SQs was not mainly controlled

470 by film diffusion and a number of other mechanisms might play an essential role in controlling

471 the rate (Oubagaranadin et al. 2007).

472 FE has been widely used for bleaching and deodorization in food and petroleum industries such

473 as bleaching of crude edible oil in the refining process (Mana et al. 2008). With this benefit, FE

474 may have potential to be used for enhanced DOC removal through a hybrid treatment process

475 where the FE can be applied after coagulation by Al-based coagulants at pH range between 5-6

476 or by Ti and Zr-based coagulants at pH range between 3-5 (Hussain et al. 2014). The practicality

477 of using FE in such a hybrid system, at much lower concentration, is a subject for further

478 investigation.

479

480 **4.   Conclusions**

481 In this study, the ability of low cost FE adsorbent to remove DOC in drinking water was

482 investigated and compared against DOC removal capabilities of MSQ and SQ. Experimental

483 results showed that FE could be highly effective for the removal of DOC. The major advantage

484 of DOC adsorption with FE was significant proportion of DOC removal at the lower dose tested

485 and at a pH level very close to neutral whereas both quartz sands performed better at a higher

486 dose and acidic pH conditions. A higher dose of FE (3 g/150 mL) showed potential to

22

487   consistently adsorb about 70% DOC even at the maximum DOC concentration of about 40

488   mg/L. EEM and HPSEC results confirmed that FE demonstrated greater removal of humic

489   compounds and low-high molecular weight compounds than SQs. The Freundlich model fitted

490   well to the adsorption data, indicating the DOC adsorption followed multi-layer formation onto

491   the FE and SQ surfaces. The adsorption kinetics was best described by the pseudo-second-order

492   model, suggesting removal mechanism followed chemisorption. Overall, the results of the

493   present study showed that FE is capable of greater DOC adsorption over a pH range 4 to 6 and at

494   comparatively low adsorbent dose over the SQs. This study demonstrates that FE is an effective

495   adsorbent for the removal of DOC in surface water treatment. Further research is suggested to

496   assess the prospective use of modified FE by thermal or chemical methods for its potential

497   application in water treatment.

498

504

505   **References**

506   Arias-Paic M, Cawley KM, Byg S, Rosario-Ortiz FL (2016) Enhanced DOC removal using

507   anion and cation ion exchange resins. Water Research 88:981-989

508   doi:http://dx.doi.org/10.1016/j.watres.2015.11.019

509   Atun G, Hisarli G, Sheldrick WS, Muhler M (2003) Adsorptive removal of methylene blue from

510   colored effluents on fuller's earth. Journal of Colloid and Interface Science 261:32-39

511   doi:http://dx.doi.org/10.1016/S0021-9797(03)00059-6

512   Bajpai AK, Vishwakarma N (2003) Adsorption of polyvinylalcohol onto Fuller's earth surfaces.

513   Colloids and Surfaces A: Physicochemical and Engineering Aspects 220:117-130

514   doi:http://dx.doi.org/10.1016/S0927-7757(03)00073-6

515   Bhatt AS, Sakaria PL, Vasudevan M, Pawar RR, Sudheesh N, Bajaj HC, Mody HM (2012)

516   Adsorption of an anionic dye from aqueous medium by organoclays: equilibrium

517   modeling, kinetic and thermodynamic exploration. RSC Advances 2: 8663-8671

518   Bonvin F, Jost L, Randin L, Bonvin E, Kohn T (2016) Super-fine powdered activated carbon

519   (SPAC) for efficient removal of micropollutants from wastewater treatment plant

520   effluent. Water Research 90:90-99 doi:http://dx.doi.org/10.1016/j.watres.2015.12.001

521   Chen W, Westerhoff P, Leenheer JA, Booksh K (2003) Fluorescence Excitation−Emission

522   Matrix regional integration to quantify spectra for dissolved organic matter.

523   Environmental Science and Technology 37:5701-5710 doi:10.1021/es034354c

524   Chow CWK, Majewski P, Bauer S, Fabris R, Drikas M (2009) Removal of natural organic

525   matter using self-assembled monolayer technology. Desalination and Water Treatment

526   12:344-351

527   Chow CWK, Fabris R, Leeuwen Jv, Wang D, Drikas M (2008) Assessing natural organic matter

528   treatability using high performance size exclusion chromatography. Environmental

529   Science and Technology 42:6683-6689 doi:10.1021/es800794r

530   Collins MR, Amy GL, Steelink C (1986) Molecular weight distribution, carboxylic acidity, and

531   humic substances content of aquatic organic matter: implications for removal during

532   water treatment. Environmental Science and Technology 20:1028-1032

533   Dastgheib SA, Karanfil T, Cheng W (2004) Tailoring activated carbons for enhanced removal of

534   natural organic matter from natural waters. Carbon 42:547-557

535   doi:http://dx.doi.org/10.1016/j.carbon.2003.12.062

536   Deegan AM, Shaik B, Nolan K, Urell K, Oelgemöller M, Tobin J, Morrissey A (2011)

537   Treatment options for wastewater effluents from pharmaceutical companies International.

538   Journal of Environmental Science and Technology 8:649-666 doi:10.1007/bf03326250

539   Fierro V, Torne-Fernandez V, Montane D, Celzard A (2008) Adsorption of phenol onto activated

540   carbons having different textural and surface properties. Microporous and Mesoporous

541   Materials 111:276-284

542   Forsberg C (1992) Will an increased greenhouse impact in Fennoscandia give rise to more humic

543   and coloured lakes? Hydrobiologia 229:51-58 doi:10.1007/BF00006990

544   Freundlich H (1926) Colloid and capillary chemistry. Methuen, London

545   Gone DL, Seidel J-L, Batiot C, Bamory K, Ligban R, Biemi J (2009) Using fluorescence

546   spectroscopy EEM to evaluate the efficiency of organic matter removal during

547   coagulation–flocculation of a tropical surface water (Agbo reservoir). Journal of

548   Hazardous Materials 172:693-699 doi:http://dx.doi.org/10.1016/j.jhazmat.2009.07.052

549   Hedegaard MJ, Albrechtsen H-J (2014) Microbial pesticide removal in rapid sand filters for

550   drinking water treatment – Potential and kinetics. Water Research 48:71-81

551   doi:http://dx.doi.org/10.1016/j.watres.2013.09.024

552 Ho YS, McKay G (2000) The kinetics of sorption of divalent metal ions onto sphagnum moss

553   peat. Water Research 34:735-742 doi:http://dx.doi.org/10.1016/S0043-1354(99)00232-8

554 Humbert H, Gallard H, Suty H, Croué J-P (2005) Performance of selected anion exchange resins

555   for the treatment of a high DOC content surface water. Water Research 39:1699-1708

556   doi:http://dx.doi.org/10.1016/j.watres.2005.02.008

557 Hussain S, van Leeuwen J, Chow CWK, Aryal R, Beecham S, Duan J, Drikas M (2014)

558   Comparison of the coagulation performance of tetravalent titanium and zirconium salts

559   with alum. Chemical Engineering Journal 254:635-646

560   doi:http://dx.doi.org/10.1016/j.cej.2014.06.014

561 Hyung H, Kim J-H (2008) Natural organic matter (NOM) adsorption to multi-walled carbon

562   nanotubes: Effect of NOM characteristics and water quality parameters. Environmental

563   Science and Technology 42:4416-4421 doi:10.1021/es702916h

564 Jarvis KL, Majewski P (2012) Plasma polymerized allylamine coated quartz particles for humic

565   acid removal. Journal of Colloid and Interface Science 380:150-158

566   doi:http://dx.doi.org/10.1016/j.jcis.2012.05.002

567 Kitis M, İlker Harman B, Yigit NO, Beyhan M, Nguyen H, Adams B (2007) The removal of

568   natural organic matter from selected Turkish source waters using magnetic ion exchange

569   resin (MIEX®). Reactive and Functional Polymers 67:1495-1504

570   doi:http://dx.doi.org/10.1016/j.reactfunctpolym.2007.07.037

571 Korth A, Fiebiger C, Bornmann K, Schmidt W (2004) NOM increase in drinking water

572   reservoirs-relevance for drinking water production. Water Supply 4:55-60

573 Lagergren S (1898) Zur Theorie der Sogenannten Absorption gelöster Stoffe. PA Norstedt &

574   söner,

575   Langmuir I (1918) The adsorption of gases on plane surfaces of glass, mica and platinum.

576   Journal of the American Chemical Society 40:1361-1403 doi:10.1021/ja02242a004

577   Matilainen A, Gjessing ET, Lahtinen T, Hed L, Bhatnagar A, Sillanpää M (2011) An overview

578   of the methods used in the characterisation of natural organic matter (NOM) in relation to

579   drinking water treatment. Chemosphere 83:1431-1442

580   doi:http://dx.doi.org/10.1016/j.chemosphere.2011.01.018

581   Matilainen A, Vepsäläinen M, Sillanpää M (2010) Natural organic matter removal by

582   coagulation during drinking water treatment: A review. Advances in Colloid and

583   Interface Science 159:189-197 doi:http://dx.doi.org/10.1016/j.cis.2010.06.007

584   Matilainen A, Vieno N, Tuhkanen T (2006) Efficiency of the activated carbon filtration in the

585   natural organic matter removal. Environment International 32:324-331

586   doi:http://dx.doi.org/10.1016/j.envint.2005.06.003

587   Oubagaranadin JUK, Sathyamurthy N, Murthy ZVP (2007) Evaluation of Fuller's earth for the

588   adsorption of mercury from aqueous solutions: A comparative study with activated

589   carbon. Journal of Hazardous Materials 142:165-174

590   doi:http://dx.doi.org/10.1016/j.jhazmat.2006.08.001

591   Perelomov L, Sarkar B, Rahman MM, Goryacheva A, Naidu R (2016) Uptake of lead by Na-

592   exchanged and Al-pillared bentonite in the presence of organic acids with different

593   functional groups. Applied Clay Science 119, Part 2:417-423

594   doi:http://dx.doi.org/10.1016/j.clay.2015.11.004

595   Rahbar MS, Alipour E, Sedighi RE (2006) Color removal from industrial wastewater with a

596   novel coagulant flocculant formulation. International Journal of Environmental Science

597   and Technology 3:79-88 doi:10.1007/bf03325910

27

598 Rusmin R, Sarkar B, Biswas B, Churchman J, Liu Y, Naidu R (2016) Structural, electrokinetic

599 and surface properties of activated palygorskite for environmental application. Applied

600 Clay Science doi: 10.1016/j.clay.2016.07.012

601 doi:http://dx.doi.org/10.1016/j.clay.2016.07.012

602 Rusmin R, Sarkar B, Liu Y, McClure S, Naidu R (2015) Structural evolution of chitosan–

603 palygorskite composites and removal of aqueous lead by composite beads. Applied

604 Surface Science 353:363-375 doi:http://dx.doi.org/10.1016/j.apsusc.2015.06.124

605 Sarkar B, Megharaj M, Xi Y, Naidu R (2011) Structural characterisation of Arquad® 2HT-75

606 organobentonites: Surface charge characteristics and environmental application. Journal

607 of Hazardous Materials 195:155-161

608 doi:http://dx.doi.org/10.1016/j.jhazmat.2011.08.016

609 Tang Y, Xu Y, Li F, Jmaiff L, Hrudey SE, Li X-F (2016) Nontargeted identification of peptides

610 and disinfection byproducts in water. Journal of Environmental Sciences 42:259-266

611 doi:http://dx.doi.org/10.1016/j.jes.2015.08.007

612 Van der Bruggen B, Vandecasteele C, Van Gestel T, Doyen W, Leysen R (2003) A review of

613 pressure-driven membrane processes in wastewater treatment and drinking water

614 production. Environmental Progress 22:46-56

615 Worrall F, Burt TP (2007) Trends in DOC concentration in Great Britain. Journal of Hydrology

616 346:81-92 doi:http://dx.doi.org/10.1016/j.jhydrol.2007.08.021

617 Yang Y, Lohwacharin J, Takizawa S (2014) Hybrid ferrihydrite-MF/UF membrane filtration for

618 the simultaneous removal of dissolved organic matter and phosphate. Water Research

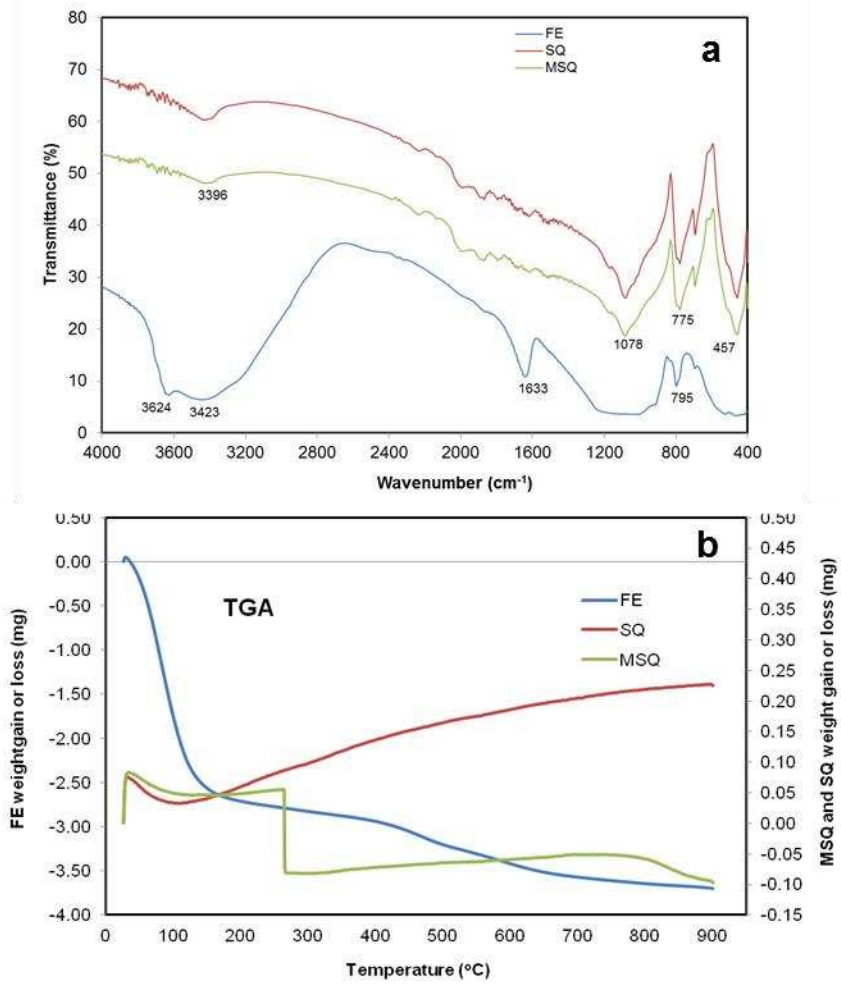619 65:177-185 doi:http://dx.doi.org/10.1016/j.watres.2014.07.030

620

621 **Figures**
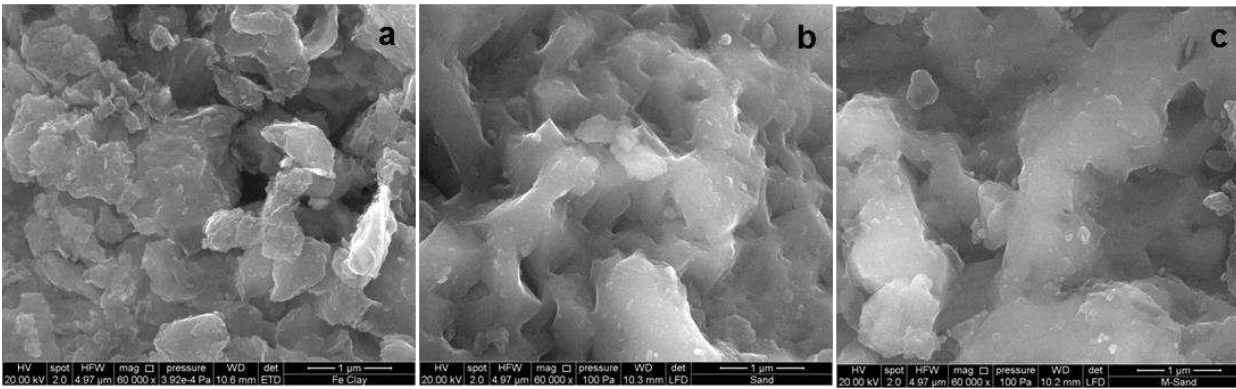
622 **Fig. 1.** SEM images of (a) fuller's earth, (b) quartz sand and (c) modified quartz sand.
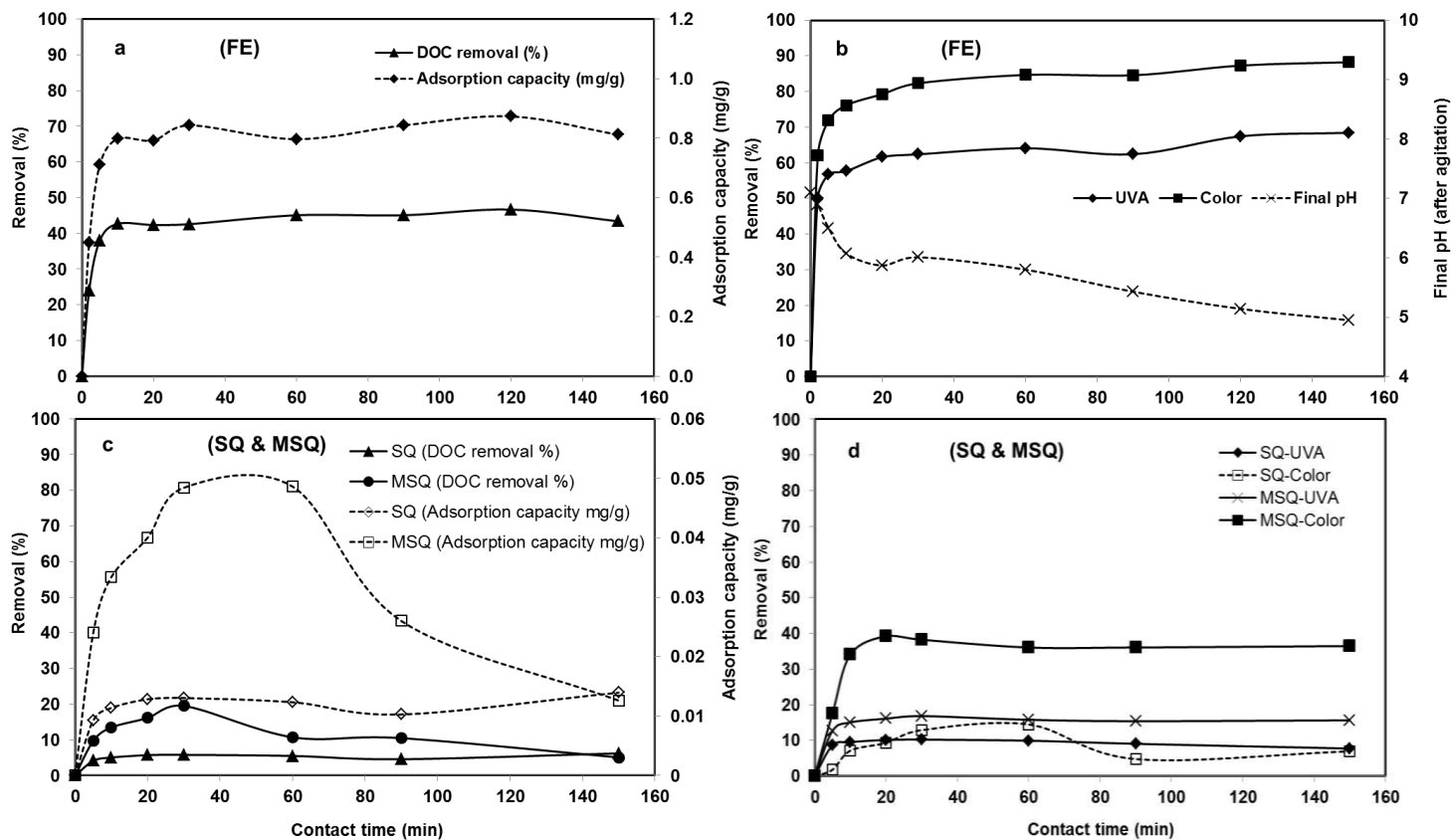
623

624

625

Fig. 2. FTIR spectra (a) and TGA plots (b) of fuller's earth (FE), quartz sand (SQ) and modified
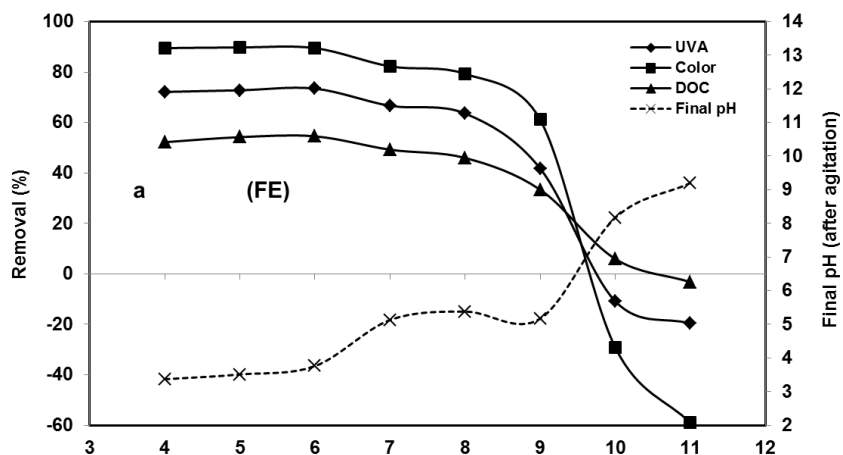
quartz sand (MSQ).

628

629

Fig. 3. Effect of contact time on the removal of DOC by (graphs a & b) fuller's earth (FE), and (graphs c & d) quartz sand with (MSQ) or without (SQ) modification. Experimental conditions: contact time range = 0-150 min; adsorbent dose = 1 g for FE and 5 g for SQs; agitation speed = 300 rpm.
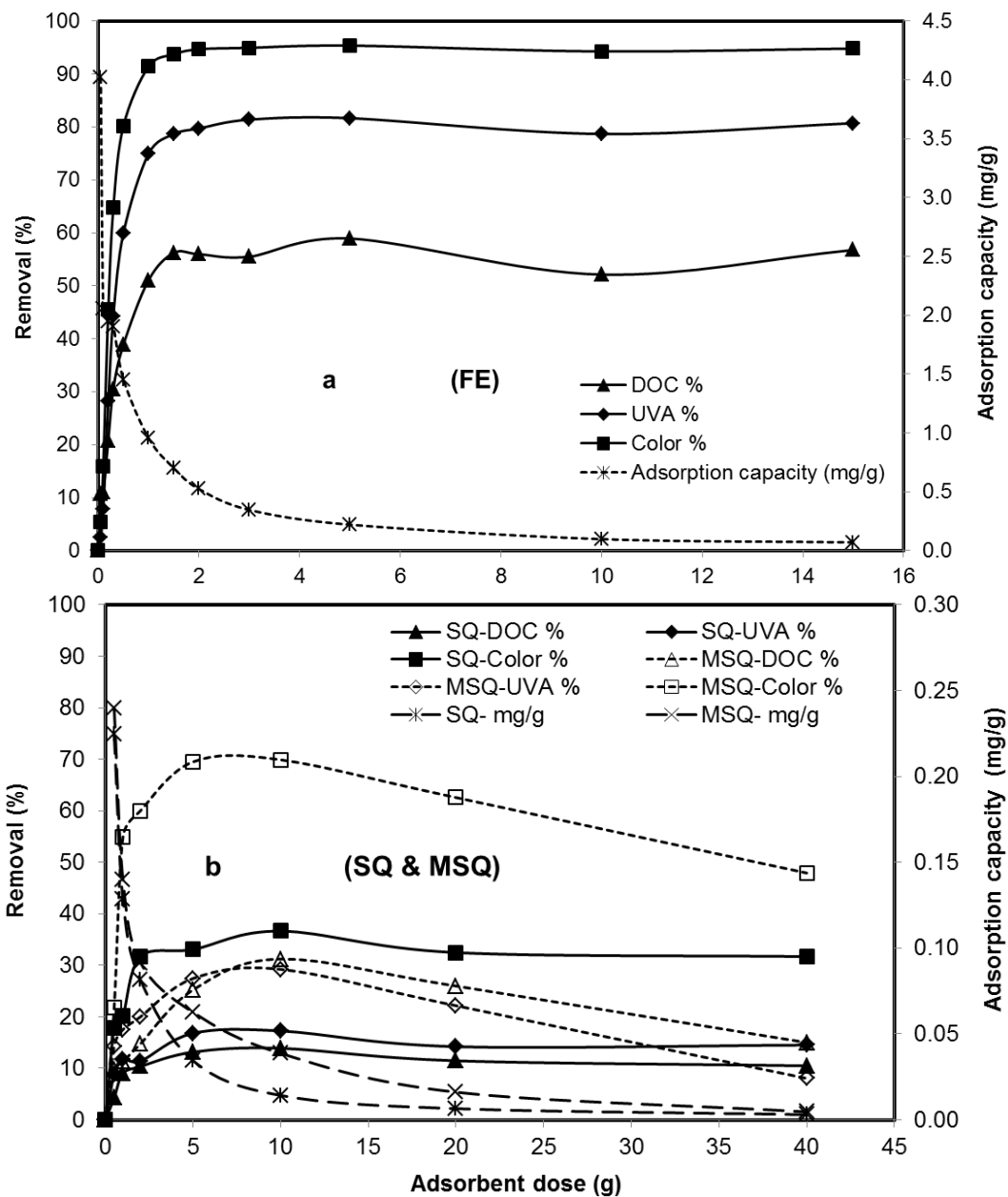
635

636

637

638
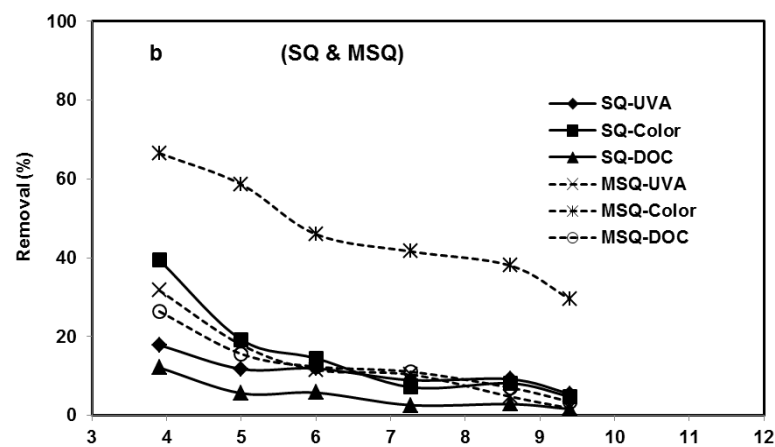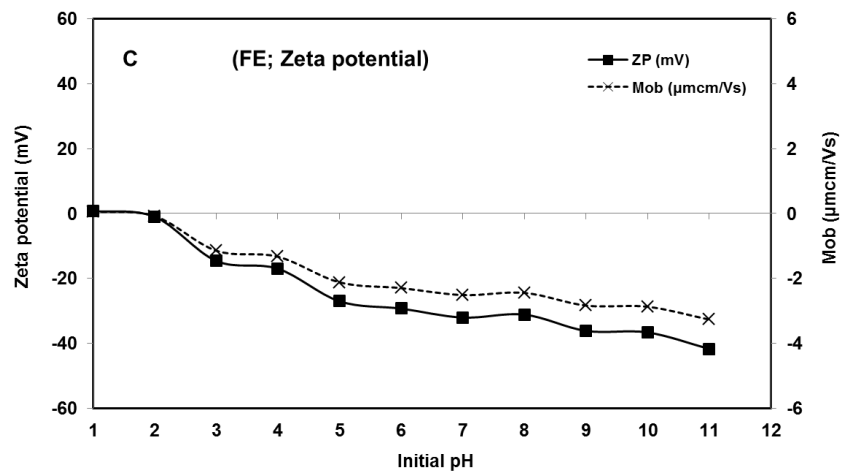
Fig. 4. Effect of pH on the removal of DOC by (a) fuller's earth (FE), (b) quartz sand with

(MSQ) or without (SQ) modification, and (c) pH-zeta potential relationship in fuller's earth

aqueous suspension. Experimental conditions: pH = 1-11; contact time = 60 min for FE and 30

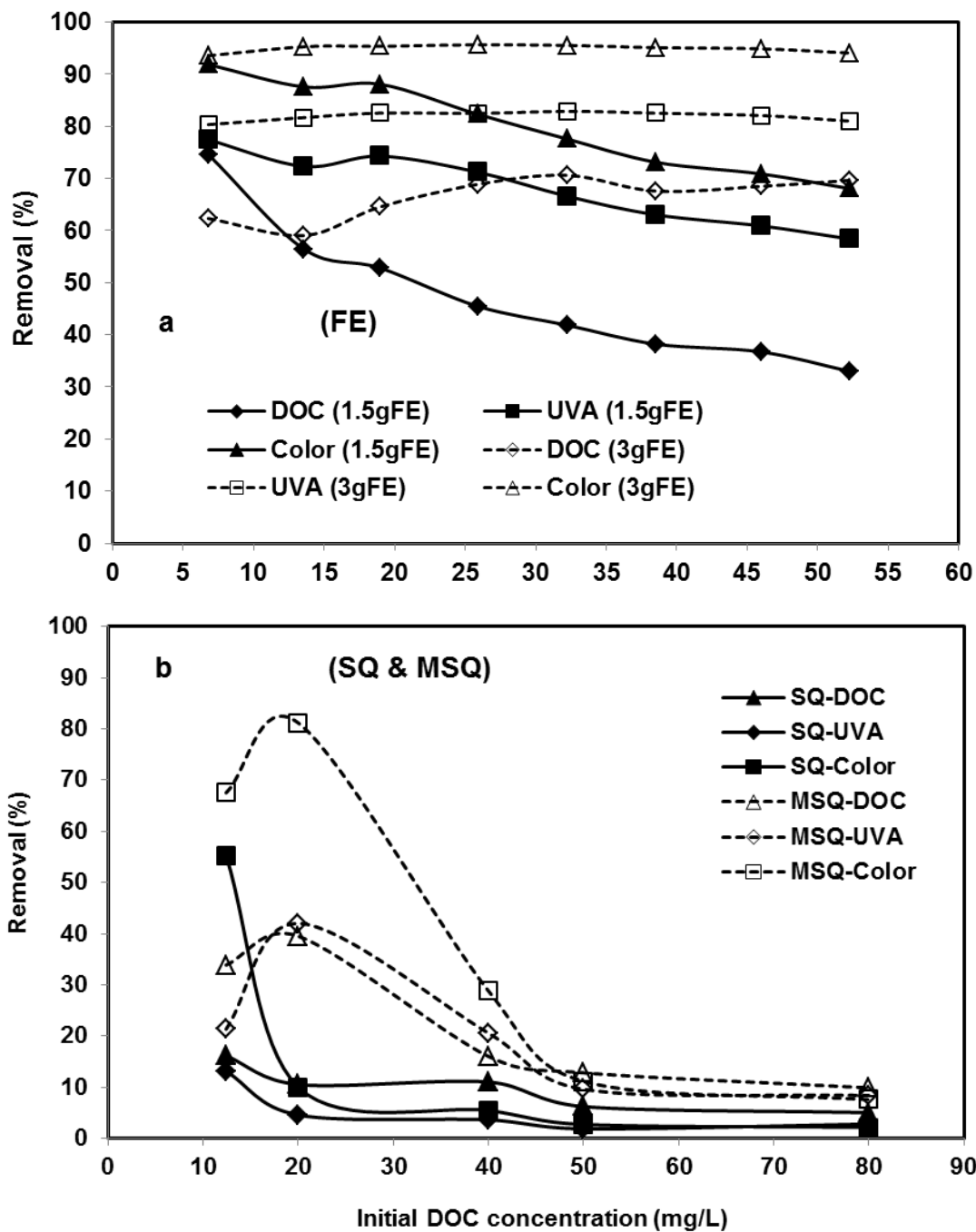min for SQs; adsorbent dose = 1 g for FE and 5 g for SQs; agitation speed = 300 rpm.

Fig. 5. Effect of adsorbent dose on the removal of DOC by (a) fuller's earth (FE), and (b) quartz sand with (MSQ) or without (SQ) modification. Experimental conditions: adsorbent dose = 0.05-15 g for FE and 0.5-40 g for quartz sand; contact time = 60 min for FE and 30 min for SQs; pH = 6 for FE and 4 for SQs; agitation speed = 300 rpm.
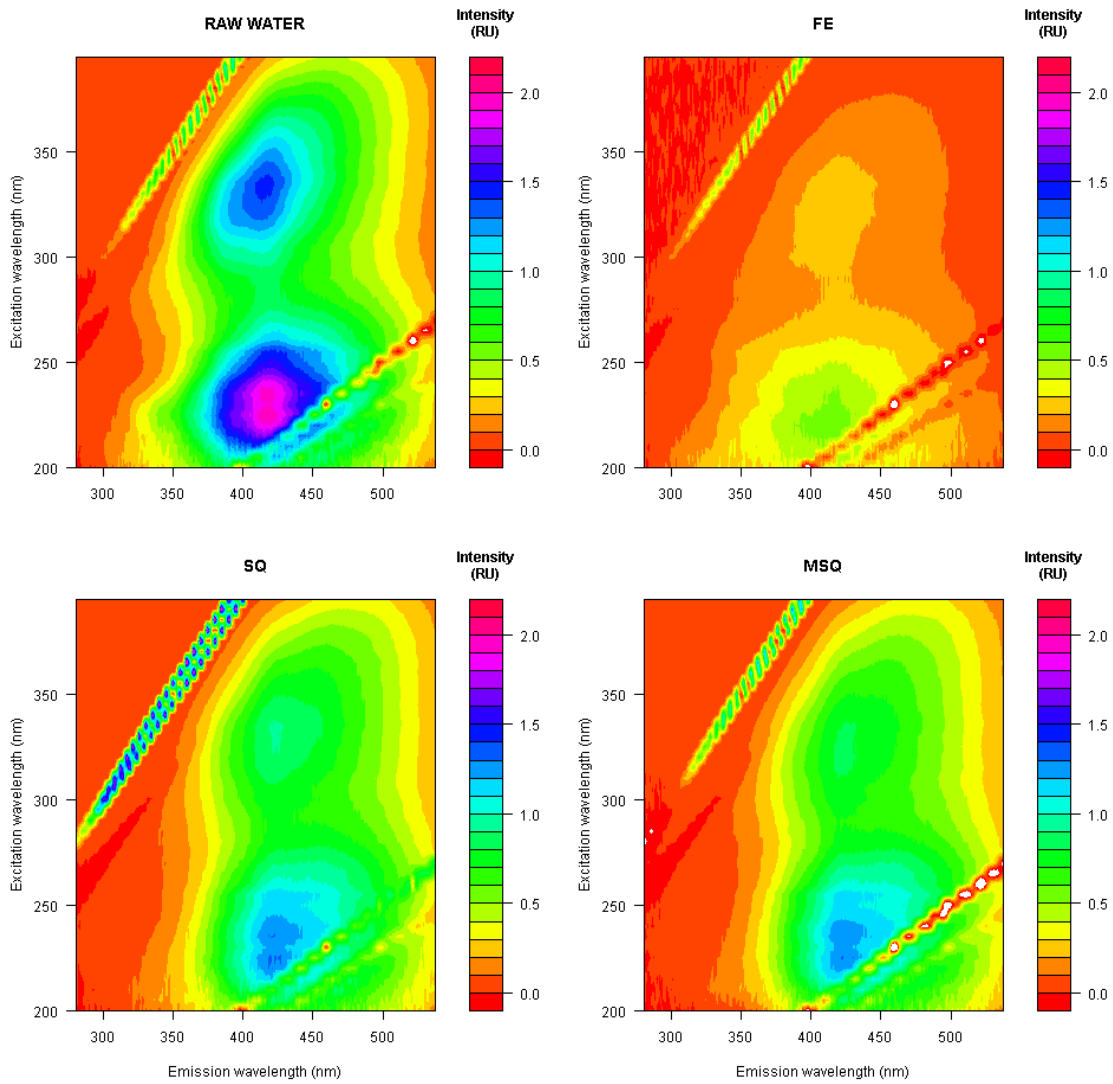
650

651

Fig. 6. Effect of initial adsorbate concentration on the removal of DOC by (a) fuller's earth (FE), and (b) quartz sand with (MSQ) or without (SQ) modification. Experimental conditions: contact time = 60 min for FE and 30 min for SQs; pH = 6 for FE and 4 for SQs; adsorbent dose = 1.5 g for FE and 10 g for SQs; agitation speed = 300 rpm.
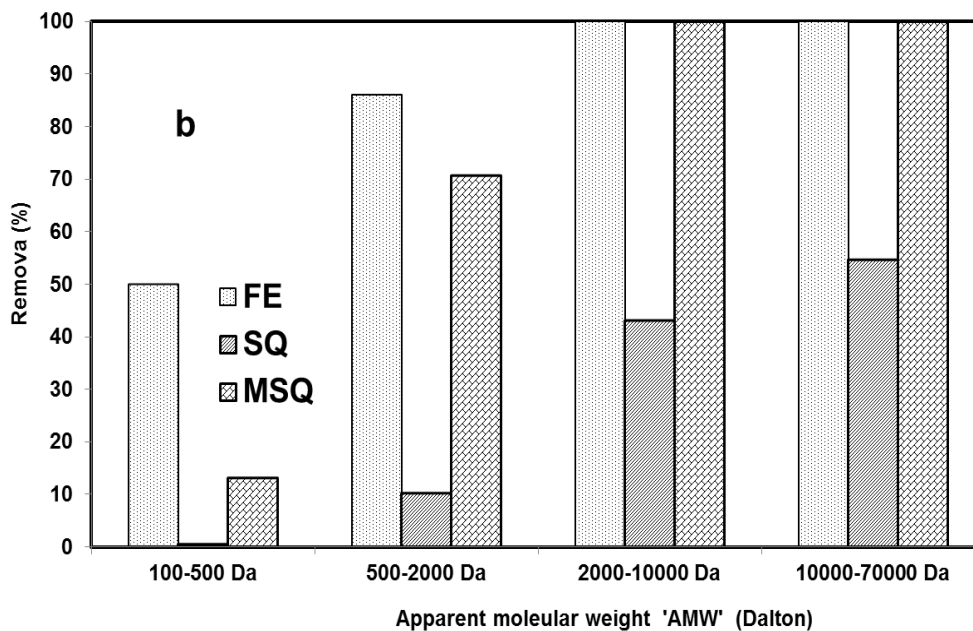
652

653

654

655

Fig. 7. 3D-fluorescence excitation-emission matrix (F-EEM) spectra of water samples before (raw) and after treatment with fuller's earth (FE) and quartz sand with (MSQ) or without (SQ) modification.

660

661
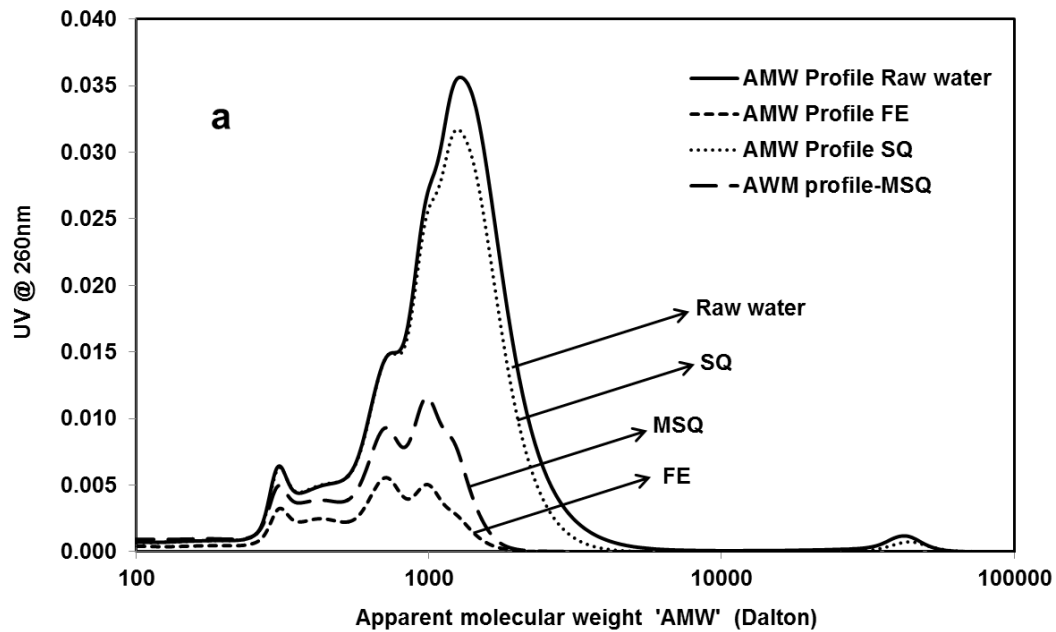
Fig. 8. High performance size-exclusion chromatography (HPSEC) based apparent molecular

weight (AMW) profiles of water samples before (raw) and after treatment with fuller's earth

(FE) and quartz sand with (MSQ) or without (SQ) modification: (a) reduction of UV 260 nm

intensity, and (b) removal efficiencies.

666

Tables

Table 1. Physiochemical properties of fuller's earth (FE), quartz sand (SQ) and modified quartz

sand (MSQ).

Parameters	FE	SQ	MSQ
Surface areas			
Single point surface area at $P/P_o = 0.30$; m²/g	227.5	0.16	0.17
BET surface area; m²/g	232.4	0.18	0.21
Langmuir Surface Area; m²/g	364.4	0.30	0.38
Pore volume			
Single point adsorption total pore volume of pores less than 27.210 Å diameter at $P/P_o = 0.300072359$; cm³/g	0.115468	0.000079	0.000088
Pore size			
Adsorption average pore width (4V/A by BET); Å	19.87	18.05	17.04
Loose bulk density; g/L	462-550		
Free moisture; (2h, 110°C) %	13.7-15		
pH (10% suspension)	2.6-3.0		
Acid content as H_2SO_4; %	0.3-0.4	-	-
Loss on ignition; %	6-7		
Loose bulk density; g/L	462		
Residue > 63 µm (%)	9-35		
Particle size; µm	60-149	430	430

672 **Table 2.** Isothermal and kinetic model parameters for the adsorption of DOC on fuller's earth (FE), modified (MSQ) and natural (SQ) quartz

673 sands.

	Isotherm models											
Adsorbent	Freundlich model			Langmuir model			Temkin model			Dubinin-Redushkevich model		
	K_f (L/mg)	n	R^2	b (mg/g)	a (L/mg)	R^2	B_1	K_T	R^2	E (J/mg)	B (mg^2/J^2)	R^2
FE	1.25×10^{-2}	0.42	0.99	-1.1320	-0.0723	0.98	4.40	0.20	0.90	223.6	0.00001	0.93
MSQ	2.13×10^{-7}	0.18	0.89	-0.0178	-0.081	0.96	1.89	3.72	0.81	100.0	0.00005	0.87
SQ	2.99×10^{-20}	0.05	0.76	-0.0036	-0.092	0.68	4.25	0.15	0.52	50.0	0.00020	0.89

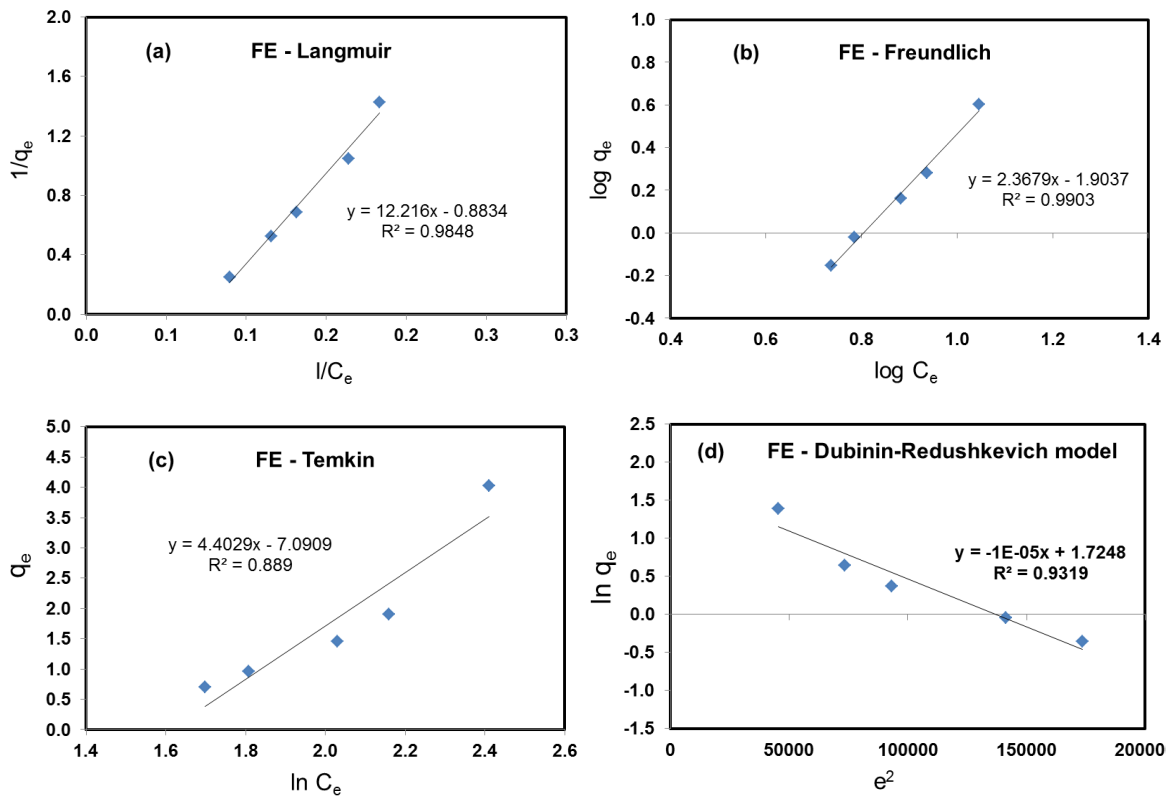|	Kinetic models								
Adsorbent	q_e (exp)	Pseudo-first-order model			Pseudo-second-order model			Intra-particle diffusion	
		q_e (cal)	R^2	K_1	q_e (cal)	R^2	K_2	R^2	K_3
	(mg/g)	(mg/g)		(min)$^{-1}$	(mg/g)		(g (mg min)$^{-1}$)		(g (mg min))
FE	0.878	0.193	0.66	0.024	0.863	0.99	0.70	0.49	0.0203
MSQ	0.049	0.028	0.82	0.008	0.054	0.99	3.11	0.84	0.0045
SQ	0.013	0.003	0.26	0.015	0.013	0.99	113.95	0.49	0.0005

674

675

676

677

678
679

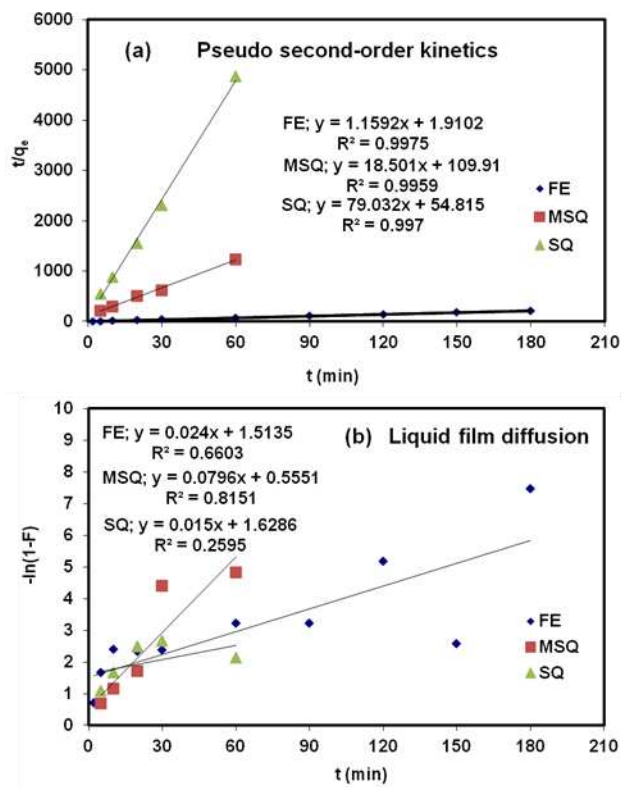680   Supplementary information:

681

682

683
684

685   **F**ig. S1. Linear fittings of DOC adsorption on fuller's earth data to various isothermal

686   models.

687

688

689

Fig. S2. Linear fittings of DOC adsorption on fuller's earth data to (a) pseudo-second-order,

and (b) liquid film diffusion models.